

The serendipitous discovery of a possible new solar system object with ALMA

W. H. T. Vlemmings^{1, *}, S. Ramstedt², M. Maercker¹, B. Davidsson²

¹ Department of Earth and Space Sciences, Chalmers University of Technology, Onsala Space Observatory, 439 92 Onsala, Sweden

² Department of Physics and Astronomy, Uppsala University, Box 516, 751 20, Uppsala, Sweden

May 18, 2018

ABSTRACT

Context. The unprecedented sensitivity of the Atacama Large millimeter/submillimeter array (ALMA) is providing many new discoveries. Several of these are serendipitous to the original goal of the observations.

Aims. We report the discovery of previously unknown continuum sources, or a single fast moving new source, in our ALMA observations. Here we aim to determine the nature of the detections.

Methods. The detections, at $> 5.8\sigma$ in the image plane and $> 14\sigma$ in the (u, v) -plane, were made in two epochs of ALMA observations of a $25''$ region around the asymptotic giant branch star W Aql in the continuum around 345 GHz. At a third epoch, covering $50'' \times 50''$, the source(s) were not seen.

Results. We have investigated if the detections could be spurious, if they could constitute a population of variable background sources, or if the observations revealed a fast moving single object. Based on our analysis, we conclude that a single object (with a flux of ~ 3.0 mJy) exhibiting a large proper motion ($\sim 87'' \text{ yr}^{-1}$) is the most likely explanation. Until the nature of the source becomes clear, we have named it *Gna*.

Conclusions. Unless there are yet unknown, but significant, issues with ALMA observations, we have detected a previously unknown objects in our solar system. Based on proper motion analysis we find that, if it is gravitationally bound, *Gna* is currently located at $12 - 25$ AU distance and has a size of $\sim 220 - 880$ km. Alternatively it is a much larger, planet-sized, object, gravitationally unbound, and located within ~ 4000 AU, or beyond (out to ~ 0.3 pc) if it is strongly variable. Our observations highlight the power of ALMA in detecting possible solar system objects, but also show how multiple epoch observations are crucial to identify what are otherwise probably assumed to be extra-galactic sources.

Key words. Minor planets, asteroids: general, Kuiper belt: general, Submillimeter: general, Proper motions

1. Introduction

Already since its first observations, the Atacama Large Millimeter/submillimeter Array (ALMA) has made many unique discoveries. For example, ALMA has revealed a galaxy with a surprisingly large amount of dust in the early Universe (Watson et al. 2015), has measured the largest Faraday rotation, indicating a strong magnetic field within light-days of a super-massive black hole (Martí-Vidal et al. 2015) and has resolved activity on the surface of an asymptotic giant branch (AGB) star (Vlemmings et al. 2015).

ALMA will also make significant progress in the study of solar system objects. In addition to observing the large planets and their moons (e.g. Cordiner et al. 2015), often used as calibrators, ALMA is a powerful tool to study the more nearby dwarf planets, asteroids or further (Extreme) Trans-Neptunian Objects, (E)TNOs (e.g. Moullet et al. 2011). Already now, in its most extended configuration, ALMA has been used to map the asteroid 3 Juno at a resolution of only ~ 60 km (ALMA Partnership et al. 2015). ALMA will thus be able to observe many solar system objects in targeted observations. However, due to the limited field of view of ALMA, it will not be an observatory that is particularly suited for large searches for new solar system bodies. Discovery of these with ALMA will likely require serendipity.

Here we report the detection of an unknown object, which is possibly a new solar system object, in our observations of the AGB star W Aql. In § 2, we describe our observations, data reduction and results. We discuss, in § 3.1, the likelihood of it being a background (extra-)galactic source. In § 3.2 we discuss the potential of it being an unbound object in our outer solar system, while in § 3.3 we describe that a gravitationally bound Centaur or TNO, currently at $10 - 20$ AU, is the more likely explanation. The conclusions are presented in § 4.

2. Observations and Results

Two epochs of observations were obtained as part of ALMA project 2012.1.00524.S (PI: Ramstedt, S.) on March 20 2014 and April 14 2014. The observational setup for the project, a 10-point mosaic uniformly covering $25''$ around the AGB stars W Aql, is described in more detail in Ramstedt et al. (2014, Ramstedt et al, in prep.). For the analysis in this paper we only used the ALMA main array observations with a resolution of $0.49'' \times 0.44''$ and maximum recoverable scale of $\sim 6''$. We did not include the Atacama Compact Array observations. The four 1.875 GHz spectral windows were, after identifying and removing line contributions, averaged to produce a continuum data set. In the images, we reached a continuum rms of 0.39 mJy beam $^{-1}$ and 0.45 mJy beam $^{-1}$ for the first and second epoch respectively. The observation on March 20 used Titan for flux calibration and

* wouter.vlemmings@chalmers.se

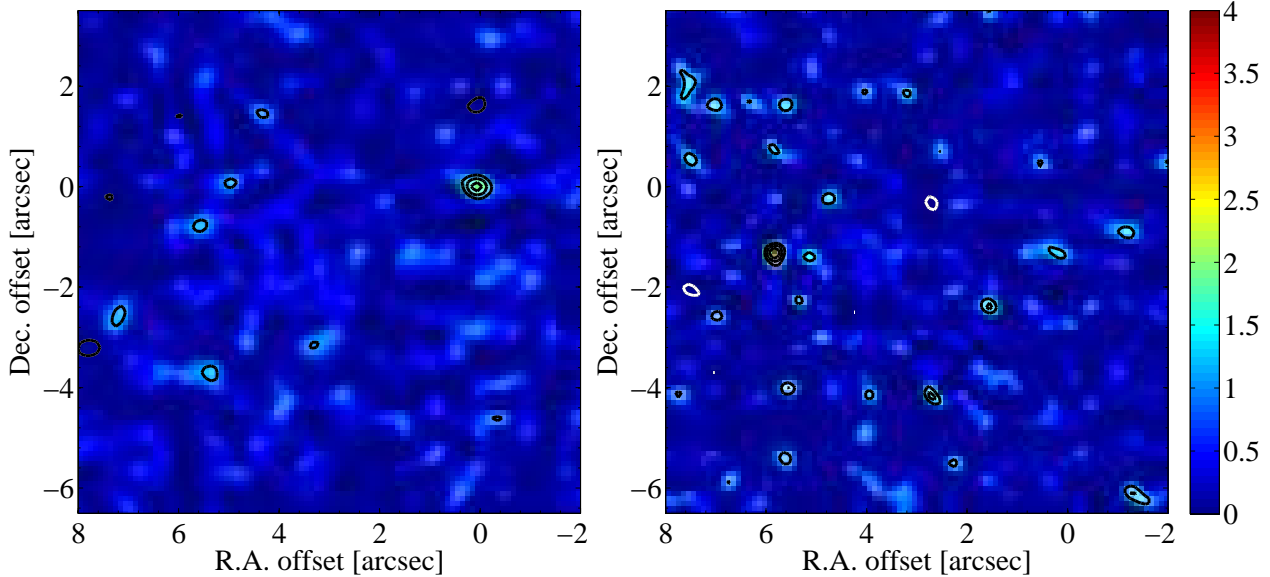


Fig. 1. The two ALMA detections at March 20 2014 (left) and April 14 2014 (right). The color scale is given in mJy beam^{-1} and the contours represent -3 (white), 3 , 4.5 , and 6σ (black). For the first epoch, $\sigma = 0.39 \text{ mJy beam}^{-1}$ and for the second epoch $\sigma = 0.45 \text{ mJy beam}^{-1}$. Before the creation of both images, the continuum of the AGB star W Aql has been subtracted in the (u, v) -plane. The $(0, 0)$ coordinate in the map corresponds to the position of the unknown source in the first epoch and has $\text{R.A.} = 19^h 15^m 23.124^s$ and $\text{Dec.} = -07^\circ 02' 48.765''$. The maps itself are centered on the position of W Aql.

the quasar J1924-2914 (2.40 Jy) for bandpass calibration. Gain calibration was performed on J1911-2006 (0.50 Jy). For the observations on April 14, J1924-2914 (2.35 Jy) was used for bandpass and flux calibration and J1911-2006 (0.51 Jy) for gain calibration.

A third epoch was taken as part of ALMA DDT observations (2012.A.00041.S, PI: Vlemmings, W.) on May 26 2014. A 39 point mosaic covering $50'' \times 50''$ around W Aql was observed in four 2 GHz continuum spectral windows centered at 338.5, 340.5, 348.5, and 350.5 GHz. The total observing time was 28 minutes and reached a point source sensitivity of $0.35 \text{ mJy beam}^{-1}$ in a $0.41 \times 0.34''$ beam. Flux and bandpass calibration was done on J1924-2914 (2.43 Jy) and gain calibration was performed using J1911-2006 (0.54 Jy). The consistent fluxes for the calibrators derived from the independently calibrated data sets indicate that the uncertainty on the flux calibration is less than $\sim 8\%$. Data processing and imaging for all epochs was performed in CASA 4.2 using standard reduction procedures.

In addition to the continuum emission from W Aql, detected at all three epochs, a clear secondary source was identified in the first two epochs. In the third epoch, the source was no longer visible above a 3σ level of 1.05 mJy . In Fig. 1, we show the images of the first two epochs, created after W Aql itself was subtracted in the (u, v) -plane. In both cases, the source was detected in the image plane at $> 5.8\sigma$. The chance detection of a source at this significance in our maps is $< 0.03\%$ based on standard Gaussian statistics using the number of independent synthesized beams in the field-of-view. However, this assumes that there are no systematic deviations from Gaussian noise properties and that cleaning of the mosaic observations has not introduced spurious sources. In order to determine the robustness of the detections, we performed a number of tests. To determine the effects of imaging the overlapping pointings of a, possibly, not completely uniform mosaic, we imaged a subset of mosaic pointings. Specifically investigating the pointings which overlap the source position, we find at both epochs that the source is detected with the expected flux in the individual pointings. We

also imaged subsets of antennas, and detect the sources (at reduced significance) in a data set with only 8 of the antennas. Finally, we fitted the sources directly in the visibility plane, using a point source model in UVMULTIFIT (Martí-Vidal et al. 2014), and find the sources are clearly detected, at even larger significance than in the image plane, with the parameters listed in Table 1. The two detections are separated by $\sim 5.9''$. We conclude that, unless there are unknown systematics in the ALMA observing system, the sources are real and the non-detection in the third epoch is significant.

3. Discussion

3.1. Background source(s)

Having established that the detections in the first two epochs are real, we proceed to discuss the possible nature of the source(s). First we consider the possibility of background sources. Cumulative submillimetre (extra-galactic) number counts at $850 \mu\text{m}$, corresponding to our observing frequency, estimate the number of submillimetre sources brighter than 2.8 mJy to be $\sim 0.7 \text{ arcmin}^{-2}$ (Knudsen et al. 2008). As the area covered in the first two epochs is only $\sim 0.14 \text{ arcmin}^2$, the expected number of background galaxies is very low. Additionally, if the sources in the two epochs are not related, a variability of at least a factor of five would be required to explain the apparent motion. The occurrence of two independently varying extra-galactic sources within such a small area is highly unlikely. This would require a large population of such objects, with a number density at least an order of magnitude larger than that of regular submillimetre source. Such a population should have been detected previously.

Considering the observed area is located $\sim 8.5^\circ$ below the Galactic plane, we also consider a Galactic origin. With no obvious indications of an extended star forming region in the direction of W Aql, nor any other nearby stellar objects that could have such a strong submillimetre emission, we rule out two in-

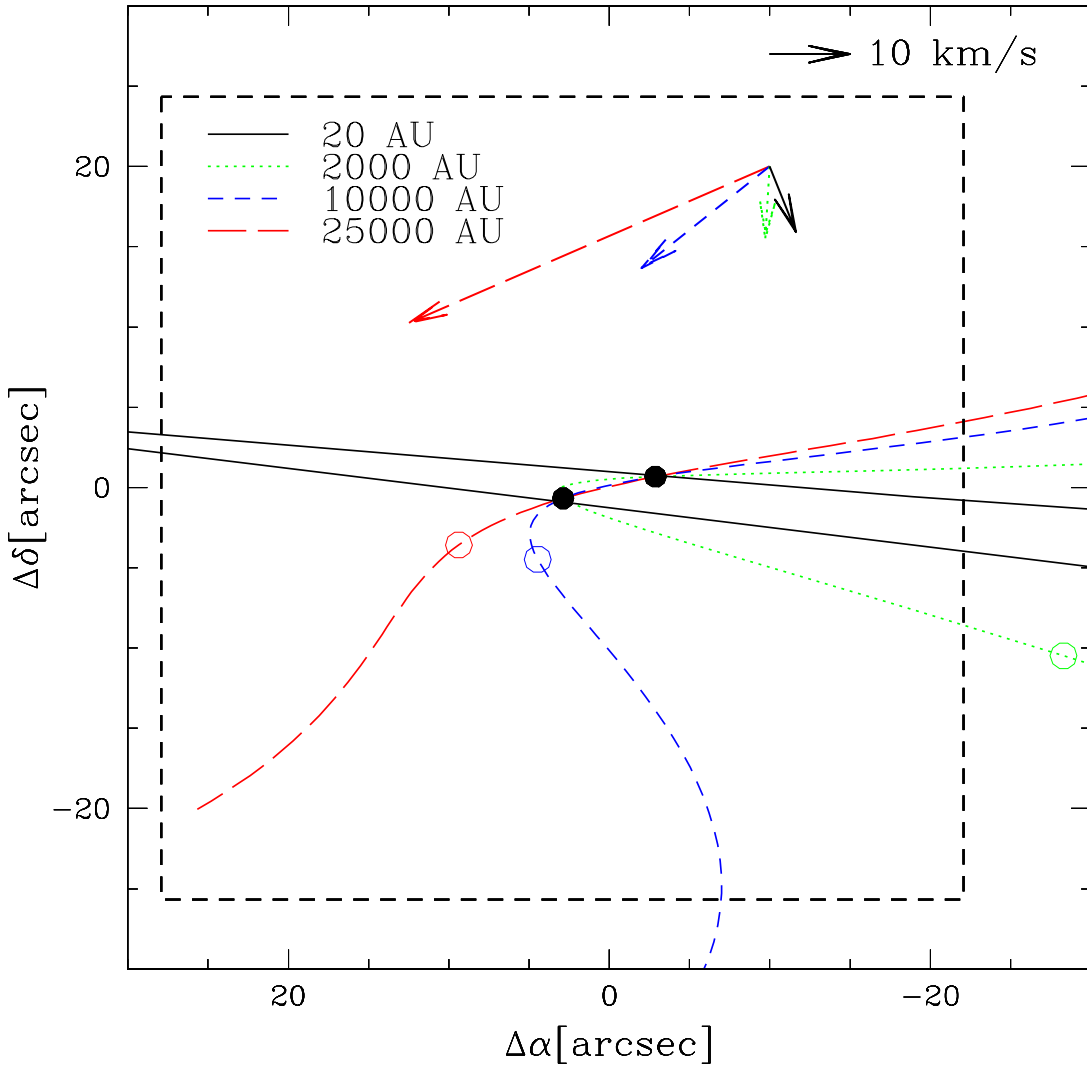


Fig. 2. Potential trajectory of motion of *Gna* based on the two ALMA detections (solid dots). The dashed square indicates the size of the third ALMA epoch mosaic in which *Gna* was not detected. The black solid line is the orbit for a source distance of $D = 20$ AU, the green short-dashed line has $D = 2000$ AU, the blue dashed line represents $D = 10000$ AU, and the red long-dashed line constitutes a source at $D = 25000$ AU. On the orbits, the open circles indicate the expected position at the epoch of the third ALMA observations. For the source at 20 AU, the expected position lies more than 1° outside the figure. The arrows denote the proper motion, scaled so that $1'' = 2 \text{ km s}^{-1}$, for each of the different orbits.

Table 1. Properties of *Gna*.

| Epoch [date] | RA [h m s.ss] | Dec [° ' "] | Flux [mJy beam⁻¹] |
|-----------------|--|------------------------------------|----------------------|
| 20-03-2014 | $19^{\text{h}} 15^{\text{m}} 23.124 \pm 0.001$ | $-07^{\circ} 02' 48.765 \pm 0.014$ | 2.8 ± 0.2 |
| 14-04-2014 | $19^{\text{h}} 15^{\text{m}} 23.534 \pm 0.001$ | $-07^{\circ} 02' 50.106 \pm 0.006$ | 3.0 ± 0.1 |
| 26-05-2014 | - | - | < 1.05 |

dependently varying Galactic background sources. As the detections in both epochs also have, within uncertainties, the same flux, we further proceed under the assumption that the two detections are the same object. To simplify the further reference to this object and acknowledge its enigmatic swift nature, we name the object *Gna* in the rest of the paper.

We now consider the case of *Gna* being a moving stellar object. Possible orbits are indicated in Fig. 2, and based on the non-detection in the third observing epoch, we can rule out an object

at > 4000 AU unless *Gna* is strongly variable. At the same time, the measured proper motion of $\sim 87'' \text{ yr}^{-1}$ would indicate a velocity of $\sim 410/D[\text{pc}] \text{ km s}^{-1}$ (ignoring the parallax contribution, see below). Such a velocity is highly unlikely for a regular stellar object beyond ~ 0.3 pc. This also immediately rules out a single object associated with the AGB star W Aql itself, as this star is located at ~ 395 pc (Danilovich et al. 2014). A distance within a few tenth of parsec would place *Gna* within the outskirts of our solar system.

3.2. A distant, gravitationally unbound, solar system source

Although the measured proper motion of *Gna* is large, it is, as seen in Fig. 2, not in the direction of the parallax motion. This contribution becomes significant already at a few tenth of a pc distance. As the parallax motion would need to be compensated by an increased proper motion to explain our two detections, the above expression for the velocity estimate becomes a lower limit and the true space velocity is shown in Fig. 3. The minimum sky velocity of *Gna* is 8.7 km s^{-1} . In Fig. 4 we indicate the Keplerian perihelion velocity, corresponding to the maximum velocity, of a gravitationally bound object with semi-major axis a . The symbols in Fig. 4 indicate the maximum current distance, based on the corresponding elliptical orbits, at which its velocity indicates *Gna* would still be gravitationally bound. It would in that case currently be located between $\sim 12 - 25 \text{ AU}$. Thus, if it is instead situated in the outer solar system, *Gna* would be unbound.

In that case, the most exciting possibility is that we have observed a planetary body or brown dwarf in the outer reaches of the Oort cloud. There have in particular been several suggestions of a large sized planetary body in the Oort cloud at over 10000 AU that may be needed to explain the apparently clustered orbits of many comets (e.g. Matese & Whitmire 2011). However, this hypothesis is strongly debated. Very recently, WISE space telescope (infrared) observations found no evidence of a planet the size of Saturn out to 28000 AU, Jupiter out to 82000 AU or a Jupiter sized brown dwarf out to 26000 AU at the locations suggested by Matese & Whitmire (Luhman 2014). A submillimetre flux of 3 mJy at a distance between 5000 – 50000 AU would indicate an object that has retained residual heat from its formation or that generates emission of its own, as it might not absorb enough solar radiation to otherwise have the measured flux. This would imply a large planet or brown dwarf and could be reconciled with the Jupiter sized brown dwarf or Saturn/Neptune size planetary limits provided by WISE (Luhman 2014), if *Gna* is located around or beyond $\sim 20000 \text{ AU}$. However, as noted above, our third epoch of observations rule out a distance to *Gna* beyond $\sim 4000 \text{ AU}$ unless it is strongly variable. Although brown dwarf variability of order $\sim 30\%$ has been observed (Robinson & Marley 2014), the submillimetre emission of the solar system planets is less (e.g. Muhleman & Berge 1991). It is thus unlikely that *Gna* is an unbound planetary body or brown dwarf beyond 4000 AU. Although we cannot rule it out to be a large unbound object within that distance, its origin and the reason for the relatively high velocity is unknown. If *Gna* is, for example, located at $\sim 100 \text{ AU}$, its flux would, assuming grey body emission with low albedo, indicate a size of almost 3500 km. Alternatively, its flux would be consistent with Neptune at approximately 2500 AU.

3.3. A nearby Centaur or trans-Neptunian object

Finally, we consider that *Gna* is gravitationally bound. In that case, Fig.4 shows that its current position is between $\sim 12 - 25 \text{ AU}$. This distance would likely indicate *Gna* to be a Centaur, with its semi-major axis between Jupiter and Neptune, or an (E)TNO. Based on this, we can constrain its size, as indicated in Fig.5. This diagram shows the size vs. distance relation for all known Centaurs as well as, for illustration, Ceres and Pluto. Considering grey-body radiation, the size of *Gna* range from $\sim 220 - 880 \text{ km}$ depending on distance and albedo. This would make it one of the largest currently known Centaurs (de la Fuente Marcos & de la Fuente Marcos 2014).

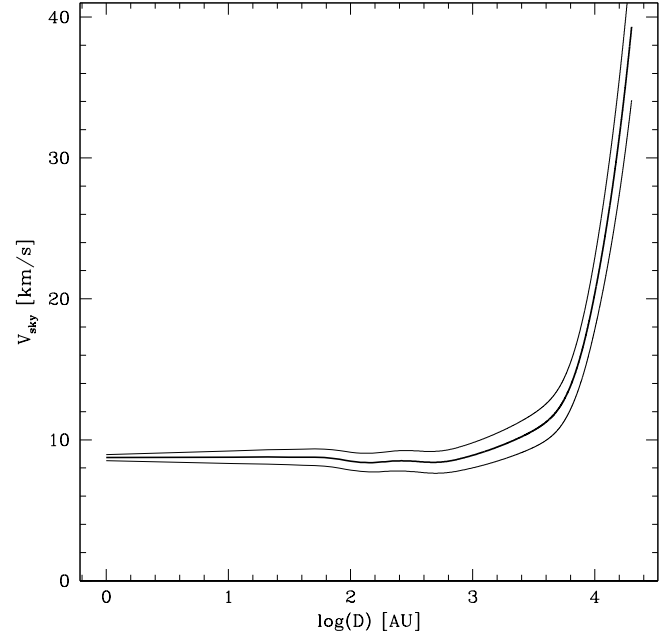


Fig. 3. The sky velocity (V_{sky}) of *Gna* for distance out to 0.1 pc. Within 10000 AU, a velocity component to compensate the parallax motion will dominate the observed motion and indicates a minimum velocity of $\sim 8.7 \text{ km s}^{-1}$. The thin lines indicate an estimate of the error envelope based on the orbit calculations.

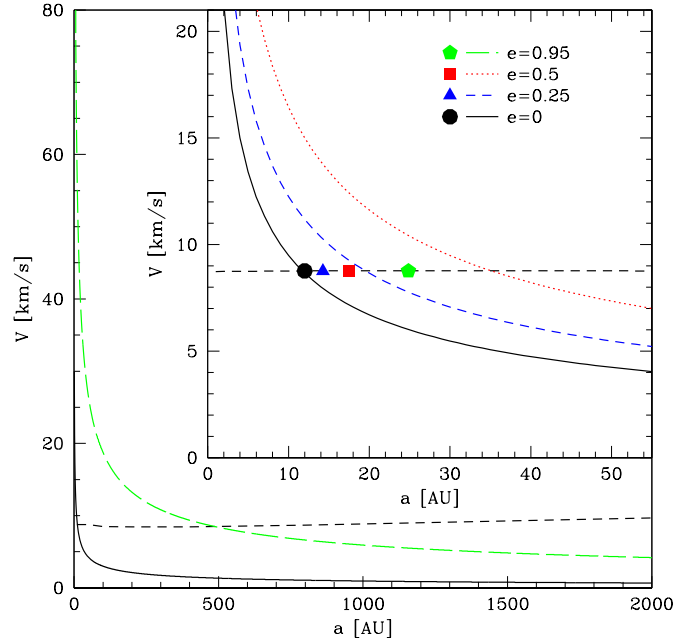


Fig. 4. The Keplerian velocity for a gravitationally bound solar system object on a circular orbit (solid black line) and the maximum velocity (at perihelion) for a gravitationally bound object on an elliptical (dotted red, dashed blue, and long dashed green lines) orbit with different eccentricity e . The velocity is given as a function of semi-major axis a . The horizontal dashed line indicates the measured velocity of *Gna*. The symbols indicate the perihelion distance at which the observed velocity corresponds to the orbital velocity for the circular and the three elliptical orbits. The circle denotes the circular orbit, the triangle the elliptical orbit with $e = 0.25$, the square the orbit with $e = 0.44$ and the pentagon the orbit with $e = 0.95$.

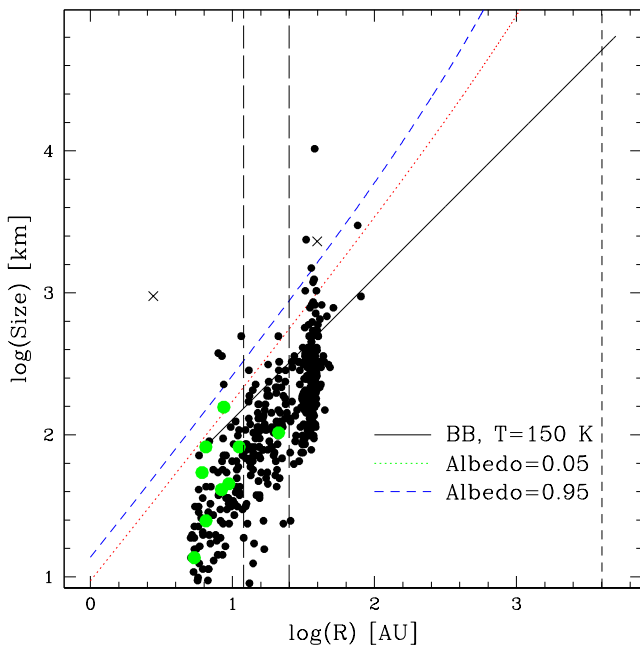


Fig. 5. The size and distances for all currently known Centaurs and scattered disc objects on prograde orbits (small black circles) and retrograde orbits (large green circles) from the minor planet center (http://www.minorplanetcenter.net/iau/lists/t_centaurs.html). Also indicated, by crosses, are Pluto and Ceres. The black solid line indicates the size-distance relation for *Gna* assuming 150 K blackbody emission. The blue dashed and red dotted line indicate the size-distance relation for *Gna* assuming grey body emission with an albedo of 0.95 and 0.05 respectively. The vertical short dashed line is the distance limit based on the orbit calculations (< 4000 AU) the vertical long dashed lines corresponds to the 12 – 25 AU distance limit if *Gna* is gravitationally bound and at a circular orbit.

As noted above and shown in Fig. 2, the parallax motion for such a nearby object is extremely large. One could thus wonder how likely it is that we would detect such an object in two observing epochs considering the small field of view. Luckily, our observations were taken exactly around the time the apparent parallax motion induced by the solar motion as seen towards W Aql reverses direction (the Sun was located in a direction almost perpendicular to the direction to W Aql), which optimizes a chance detection.

The orbit calculations indicate that at $\sim 12 - 25$ AU, the orbital motion is retrograde with an inclination of $\sim 120^\circ$, and *Gna* is currently within $\sim 10^\circ$ of the ecliptic. This would make *Gna* a member of the subclass of retrograde Centaurs, which are thought to be objects on unstable orbits brought in from the Oort cloud (Volk & Malhotra 2013; de la Fuente Marcos & de la Fuente Marcos 2014). As shown in Fig. 5, *Gna* would be the largest member of this class.

Considering its size, the main question regarding this possible classification is why *Gna* was not detected previously, as no previously known object was found to be within 1' of W Aql during our observations¹. The most likely explanation would be that the location of W Aql close to the Galactic plane ($b = -8.5^\circ$) has been avoided by most surveys (e.g. Sheppard et al. 2011) in order to avoid confusion.

The best way to confirm the Centaur/(E)TNO hypothesis will be timed observations at a variety of wavelength of the region

around W Aql at dates very close to the dates at which *Gna* was detected with ALMA.

4. Conclusions

Based on our three epochs of ALMA observations around 345 GHz we conclude that:

- Continuum observations robustly detected point-like emission at the level ~ 3 mJy at different positions in two epochs separated by 25 days. Unless an unknown systematic effect in ALMA observations can routinely produce $> 5.8\sigma$ detections, we confirm the detections as real. In the unlikely case that the effect is spurious, our observations highlight the very strong need for multiple epochs of ALMA observations to confirm new source detections.
- The consistency of the flux and the negligible probability of having identified two independent highly variable background sources, leads us to conclude the two detections are the same source, here dubbed *Gna*. The source was no longer visible at the third epoch another 42 days later.
- Based on the motion of almost 6" between the two epochs, we can rule out a source beyond ~ 0.3 pc. Assuming *Gna* is not strongly variably, the lack of detection in the third epoch confines it to within ~ 4000 AU. Only if it is variable by more than a factor of ~ 5 , could *Gna* be a large planetary body or brown dwarf beyond that distance in the outer solar system.
- The observations can not rule out an gravitationally unbound large solar system object within ~ 4000 AU. The detection at only two of the three epochs and the flux would be consistent with Neptune at ~ 2500 AU.
- Assuming it is gravitationally bound, the most likely explanation is that *Gna* belongs to the small group of large retrograde Centaurs or trans neptunian objects. In that case *Gna* is currently at $\sim 12 - 25$ AU, and has a size between 220 – 880 km.

Acknowledgements. This paper makes use of the following ALMA data: ADS/JAO.ALMA#2012.1.00524.S and ADS/JAO.ALMA#2012.A.00041.S. ALMA is a partnership of ESO (representing its member states), NSF (USA) and NINS (Japan), together with NRC (Canada) and NSC and ASIAA (Taiwan) and KASI (Republic of Korea), in cooperation with the Republic of Chile. The Joint ALMA Observatory is operated by ESO, AUI/NRAO and NAOJ. WV acknowledges support from VR, a Marie Curie Career Integration Grant 321691, and the ERC consolidator grant 614264. M.M. has received funding from the People Programme (Marie Curie Actions) of the EU's FP7 (FP7/2007-2013) under REA grant agreement No. 623898.11. We also thank Prof. Spahr from the Minor Planet Center for helpful discussion and the JAO and ESO ARC staff for promptly scheduling the DDT observations.

References

- ALMA Partnership, Hunter, T. R., Kneissl, R., et al. 2015, ApJ, 808, L2
- Cordiner, M. A., Palmer, M. Y., Nixon, C. A., et al. 2015, ApJ, 800, L14
- Danilovich, T., Bergman, P., Justtanont, K., et al. 2014, A&A, 569, A76
- de la Fuente Marcos, C. & de la Fuente Marcos, R. 2014, Ap&SS, 352, 409
- Knudsen, K. K., van der Werf, P. P., & Kneib, J.-P. 2008, MNRAS, 384, 1611
- Luhman, K. L. 2014, ApJ, 781, 4
- Marti-Vidal, I., Muller, S., Vlemmings, W., Horellou, C., & Aalto, S. 2015, Science, 348, 311
- Marti-Vidal, I., Vlemmings, W. H. T., Muller, S., & Casey, S. 2014, A&A, 563, A136
- Matese, J. J. & Whitmire, D. P. 2011, Icarus, 211, 926
- Mouillet, A., Lellouch, E., Moreno, R., & Gurwell, M. 2011, Icarus, 213, 382
- Muhleman, D. O. & Berge, G. L. 1991, Icarus, 92, 263
- Ramstedt, S., Mohamed, S., Vlemmings, W. H. T., et al. 2014, A&A, 570, L14
- Robinson, T. D. & Marley, M. S. 2014, ApJ, 785, 158
- Sheppard, S. S., Udaliski, A., Trujillo, C., et al. 2011, AJ, 142, 98
- Vlemmings, W. H. T., Ramstedt, S., O'Gorman, E., et al. 2015, A&A, 577, L4
- Volk, K. & Malhotra, R. 2013, Icarus, 224, 66
- Watson, D., Christensen, L., Knudsen, K. K., et al. 2015, Nature, 519, 327

¹ <http://www.minorplanetcenter.net/cgi-bin/mpcheck.cgi>